Journal of Materials Chemistry C

Accepted Manuscript

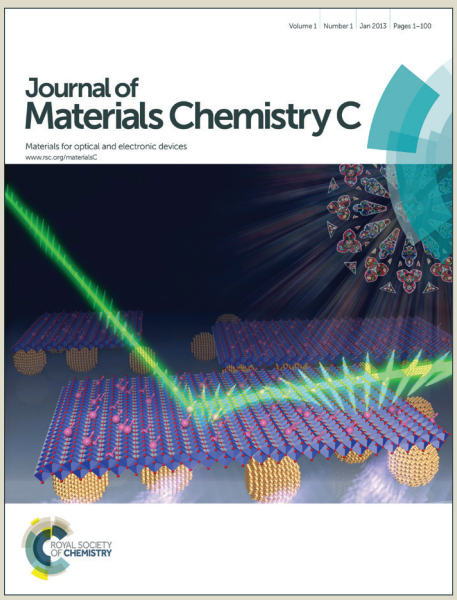

ROYAL SOCIETY OF CHEMISTRY

www.rsc.org/materialsC

ARTICLE TYPE www.rsc.org/xxxxxx | XXXXXXXX

Ordered and Flexible Lanthanide Complex Thin Films Showing Up-conversion and Color-tunable Luminescence

Rui Gao,[a] Minjun Zhao,[a] Yan Guan,[c] Xiaoyu Fang,[a] Xiaohong Li,[a] and Dongpeng Yan,*[,ab]

Received (in XXX, XXX) Xth XXXXXXXXX 200X, Accepted Xth XXXXXXXXX 200X
First published on the web Xth XXXXXXXXX 200X
DOI: 10.1039/b000000x

The polarized and up-conversion luminescent films have great potential for use in the design of various optical devices. In this work, we report the transparent and flexible thin films based on alternate layer-by-layer assembly of sulfonated Eu- and Tb-based lanthanide complexes (LCs) and Mg–Al-layered double hydroxide (LDH) nanosheets. UV-visible absorption and fluorescence spectroscopy showed an orderly growth of the two types of thin films (TFs) upon increasing the number of deposition cycle. XRD, AFM and SEM measurements indicated that the films feature periodic layered structures as well as uniform surface morphology. Moreover, by combining the assembly of both the Eu- and/or Tb-based LC systems, these TFs can exhibit well-defined one- and two-color polarized fluorescence with high polarization anisotropy. In addition, it was observed that the two TFs exhibited obvious red and green up-conversion emission upon excited by a near-IR laser light. Therefore, this work provides a facile way to develop new types of LC TFs with both up-conversion and color-tunable luminescence, which have much potential applications for the design of various LC-based optical films and flexible devices.

1. Introduction.

Lanthanide ions own fascinating optical properties due to their unique *f-f* electronic transitions in contrast to pure organic phosphors[1a,b] and inorganic quantum dots.[1c] They have been widely investigated in view of their potential applications in biological labeling,[2a] light emitting diodes,[2b] and molecular devices.[2c] Furthermore, combining the advantages of high luminescent efficiency and color purity of lanthanide ions with the low excitation energy, high absorption efficiency and tailorable molecular structure of organic ligands, lanthanide complexes (LCs) can be effectively applied into both photoluminescence (PL) and electroluminescence (EL) systems.[3a-d] To date, many LCs have been continuously reported, some challenges remain unresolved however.[4a,b] For example, the development of highly ordered luminescent LC film materials is important for their future optoelectronic applications in the display field, whereas such LC-based films are still difficult to be fabricated and have been much less studied compared with the pure organic and polymer systems.[4c] Furthermore, although the up-conversion luminescence based on the lanthanide-doped nanocrystal materials are widely used and developed,[5a-d] there are still very few examples of LC materials with high-efficiency up-conversion emission.[5e,f] Such materials may find new applications in near-infrared detection and wavelength-transfer image.[6a,b] In addition, to meet the requirements of next generation optical displays, the construction of new multi-color luminescent systems in desirable regions by combination of different color-emissive LC materials continues a major goal.[6c,d]

Layered double hydroxides (LDHs) are one type of layered solid host matrix, which have been widely used in the areas of catalysis,[7a] biology,[7b] and optical materials.[7c-e] They can be described by the general formula $[M^{II}_{1-x}M^{III}_{x}(OH)_2]^{z+}A^{n-}_{z/n}\cdot yH_2O$. M^{II} and M^{III} are divalent and trivalent metals respectively; A^{n-} is the anion.[8a,b] Recently, the development of techniques for the delamination of LDH microcrystals into LDH nanosheets (Scheme 1a) paves a useful way to fabricate nanostructured films.[8c-f] Particularly, the LDH-based luminescent thin films (TFs) can be fabricated based on the alternate layer-by-layer (LBL) of positive-charged LDH nanosheets and fluorescent anions, which exhibit controllable thickness and uniform emission intensity. Moreover, the optical stability of the chromophores confined within LDH layers can be improved because of the host–guest interactions. In principle, based on the electrostatic co-assembly of the fluorescent molecules with different emissive wavelength and LDH nanosheets, it can be possible to fabricate tunable multi-color luminescent TF systems due to the regular orientation of the different fluorescent molecules within the 2D LDH matrix.[8] Up to now, although several types of fluorescent anions (such as polymer,[9a] Ru-based complex,[9b] and small molecule[9c]) have been successfully assembled with LDH to obtain nanocomposites, the construction of ordered LC/LDH films is still rarely reported.[5]

With the development of both highly uniform LC-based films and multi-color emissive systems in mind, herein, we have synthesized the sulfonated Eu(III)- and Tb(III)-based complexes (Scheme 1b and 1c) and Mg-Al--LDH nanosheets as the basic building blocks. This facilitates the assembly of a new type of functional hybrid film which combines the properties of the LCs with those of the inorganic component, and the obtained TFs can present uniform red/green emission by using the LBL method (Scheme 1d). By rational choosing suitable substrates, the rigid and flexible LC-based TFs can be obtained. The resulting TF systems present long-range ordered structure, polarized anisotropy, up-conversion luminescence as well as improved photoluminescent quantum yield (PLQY) and fluorescence

lifetime compared to their solution and powder counterparts. Moreover, the alternate deposition or co-assembly of two types of LCs with LDH nanosheets also affords the tunable two-color luminescent films. Therefore, this work provides a viable methodology for fabricating ordered LC-based TFs by the incorporation of LC molecules into 2D inorganic layers, which can be potentially applied in flexible multi-color displays, polarized luminescence and up-conversion emission.

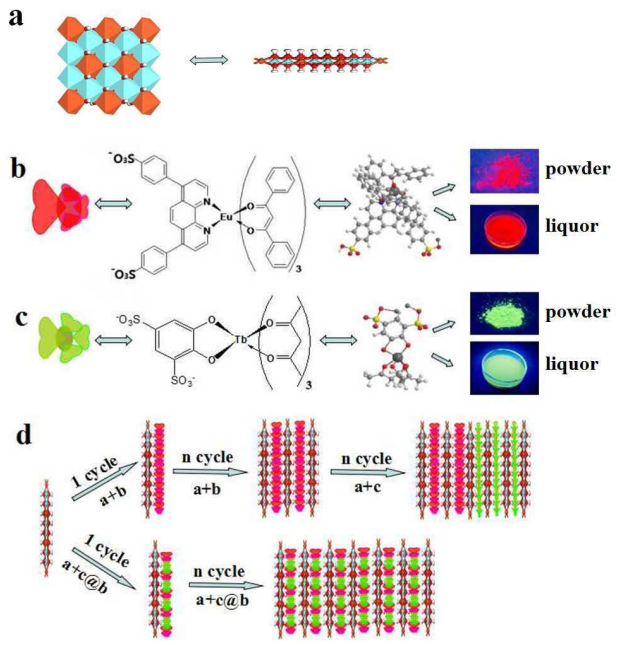

Scheme 1. a) the monolayer of Mg-Al-layered double hydroxide (Mg-Al-LDH) (dark orange: $Al(OH)_6$ octahedra; blue: $Mg(OH)_6$ octahedra); the chemical formula of b) $Eu(DBM)_3bath$ (red luminescence), c) $Tb(acac)_3Tiron$ (green luminescence), insets in b) and c) show the red/green fluorescence of the powder and solution (10^{-4} mol/L) forms; d) procedures for assembling one-/two-color luminescent TFs.

2. Experimental Section.

2.1 Reagents and materials.

Europium (□) chloride ($EuCl_3$), terbuium (□) chloride ($TbCl_3$), 2,4-pentanedione (acac), dibenzoylmethane (DBM), 4,5-dihydroxy-1,3-benzenedisulfonic acid disodium salt (Tiron) and bathophenanthroline disulphonic acid disodium salt trihydrate (bath) were purchased from J&K Chemical Co. Ltd. Analytical grade $Mg(NO_3)_2{\cdot}6H_2O$, $Al(NO_3)_3{\cdot}9H_2O$ and urea were purchased from Beijing Chemical Co. Ltd. and used without further purification.

2.2 Synthesis of $Eu(DBM)_3bathCl_3Na_2$ and $Tb(acac)_3TironCl_3Na_2$ LCs.

$Eu(DBM)_3bathCl_3Na_2$ was prepared as follows: typically, 1 mmol of $EuCl_3$ was dissolved into 10 mL of deionized water, 3 mmol of DBM was dissolved into 20 mL of ethanol, and 1 mmol of bath was dissolved in 10 mL of deionized water. The DBM solution was poured into the $EuCl_3$ solution firstly, and the pH value of the mixed solution was then adjusted to 6.5. Subsequently, the bath solution was dropwise added into the mixed solution, which was further stirred at 60 °C. After 1 h, the yellow precipitate can be obtained, which was further deposited and collected by centrifugation. The precipitate was dried at 65 °C. The synthesis process of $Tb(acac)_3TironCl_3Na_2$ is similar to that described in the synthesis of $Eu(DBM)_3bathCl_3Na_2$. The yields for the reactions are 79.86% for $Eu(DBM)_3bathCl_3Na_2$ and 82.94% for $Tb(acac)_3TironCl_3Na_2$.

2.3 Fabrication of the one- and two-color luminescent TFs.

The processes of synthesis and exfoliation of Mg-Al-LDH were similar to that described in our previous work.[10] 0.1 g of Mg-Al-LDH was shaken in 100 cm^3 of formamide for 24 h to produce a colloidal suspension of exfoliated Mg-Al-LDH nanosheets. The quartz glass substrate was cleaned in concentrated NH_3/30% H_2O_2 (7:3) and concentrated H_2SO_4 for 30 min each. After each procedure, the quartz substrate was washed thoroughly with deionic water. The substrate was dipped in a colloidal suspension (1 g L^{-1}) of LDH nanosheets for 10 min followed by washing thoroughly, and then the substrate was treated with a 50 mL of LC ($Eu(DBM)_3bath$ or $Tb(acac)_3Tiron$) aqueous solution (1 mmol/L) for 10 min. The multilayer $(LC/LDH)_n$ TFs were fabricated by alternate deposition of LDH nanosheets suspension and LC solution for *n* cycles. Fabrication of the two-color luminescent TFs involved the alternate deposition of one type of luminescent TF onto the surface of a different as-prepared luminescent TF. By controlling the deposition sequence and number of layer-by-layer cycles, TFs with two-color luminescence were obtained. The as-prepared $(Eu(DBM)_3bath/LDH)_{10}$ TF with $Eu(DBM)_3bath$ as the top layer was dipped into a colloidal suspension (1 mmol/L) of LDH nanosheets for 10 min and then washed thoroughly. The resulting TF was immersed into a 100 mL of $Tb(acac)_3Tiron$ aqueous solution (1 mmol/L) for another 10 min and then washed. Multilayer films of $(Eu(DBM)_3bath/LDH)_{10}/(Tb(acac)_3Tiron/LDH)_n$ (n=0-14) were fabricated by alternate deposition into a suspension of LDH nanosheets and a solution of $Tb(acac)_3Tiron$ for *n* cycles. The resulting films were dried under a nitrogen gas flow for 2 min at 25 °C. Other two-color systems can be constructed by another process. For example, the $(Eu(DBM)_3bath@Tb(acac)_3Tiron/LDH)_{10}$ (c=0–35%) was fabricated by alternate deposition of the suspension of LDH nanosheets and the mixed $Eu(DBM)_3bath@Tb(acac)_3Tiron$ solution for 10 cycles (c=0–35%, which stands for the molar ratio of $Eu(DBM)_3bath$ to $Tb(acac)_3Tiron$).

2.4 Sample characterization.

The UV-vis absorption spectra were collected in the range from 190 to 900 nm on a Shimadzu U-3000 spectrophotometer, with the slit width of 1.0 nm. The FT-IR spectra were used on AVATAR-370 FT-IR with the range from 400 to 4000 cm^{-1}. The fluorescence spectra were performed on RF-5301PC fluorospectrophotometer with the excitation wavelength of 310 and 360 nm, and both the excitation and emission slit were set to 1 nm. Steady-state polarized photoluminescence and fluorescent lifetime measurements were recorded with an Edinburgh Instruments' FLS 980 fluorospectrophotometer. X-ray diffraction

patterns (XRD) of TFs were recorded using a Rigaku 2500VB2+PC diffractometer under the conditions: 40 kV, 50 mA, Cu Kα radiation (λ = 0.154056 nm) with step-scanned in step of 0.04° (2θ) in the range from 2 to 10° using a count time of 10 s/step. The C, H, N, S elemental analysis was measured using the varioELcube instrument. The mass spectra (MS) of the LCs was obtained by using an Micromass Quattro premier. The morphology was investigated by using a scanning electron microscope (SEM Hitachi S-3500) equipped with an EDX attachment (EDX Oxford Instrument Isis 300), and the accelerating voltage applied was 20 kV. The surface roughness and thickness data were obtained by using the atomic force microscopy (AFM) software (Digital Instruments, Version 6.12). Photoluminescence quantum yield (PLQY) was measured using an HORIBA Jobin Yvon FluoroMax-4 spectrofluorimeter, equipped with an F-3018 integrating sphere. Up-conversion fluorescence of the samples was excited by an 800 nm laser on a Tsunami-Spit-fire-OPA-800C ultrafast optical parameter amplifier (Spectra-Physics).

3. Results and Discussion.

3.1 Characterizations of the LCs.

The ligands of the water-soluble Eu(III)- and Tb(III)-based complexes are DBM/bath (dibenzoylmethane/bathophenanthroline disulfonate disodium) and acac/Tiron (2,4-pentanedione/4,5-dihydroxy-1,3-benzenedisulfonate disodium) respectively. FT-IR spectra (Fig. S1 in Electronic Supplementary Information (ESI)) show that the as-prepared LCs present the characteristic peaks of their first and second ligands. The C, H, N, S elemental analysis and mass spectra (MS, Fig. S3 in ESI) were also performed on the as-prepared complexes. By contrasting the elemental analysis of experimental and theoretically calculated results for two LC systems (Table S1 in ESI), it can be known that the experimental molecular formula for two LC systems are consistent well with those of the theoretical ones. In addition, both the Eu(DBM)$_3$bath and Tb(acac)$_3$Tiron solutions and powders exhibit well-defined red and green fluorescence (Scheme 1b and 1c, CIE 1931 color coordination: (0.71, 0.29) and (0.33, 0.60)), which exhibit the characteristic emissive peaks of Eu(III)- and Tb(III)- complexes at 581 nm ($^5D_0 \rightarrow {}^7F_0$), 614 nm ($^5D_0 \rightarrow {}^7F_2$) and 488 nm ($^5D_4 \rightarrow {}^7F_6$), 544 nm ($^5D_4 \rightarrow {}^7F_5$), respectively (Fig. S2a and S2b in ESI).

3.2 Fabrication of the one-color LCs/LDH TFs.

The fabrication of the LC-based TFs involves the alternate dipping a quartz substrate into colloidal LDH nanosheets and the Eu(III) or Tb (III) LC solutions. UV-vis absorption measurement was employed to monitor the assembly process of the (LC/LDH)$_n$ TFs (Fig. 1). The characteristic absorption bands of (Eu(DBM)$_3$bath/LDH)$_n$ and (Tb(acac)$_3$Tiron/LDH)$_n$ can be observed at 288 nm (π-π* transition of bath) and 219 nm ($^1E_{1u}$ transition of Tiron), respectively, whose intensity correlates linearly with the number of bilayer (n) (Fig. 1a and 1b, inset), demonstrating an ordered and regular film growth procedure. The photograph of the TFs under daylight (inset in Fig. 1) provides a visual verification of the transparence of the TFs with different n. In addition, The TFs also exhibit the characteristic fluorescent emission at *ca.* 581 nm, 614 nm and *ca.* 488 nm, 544 nm with enhanced intensity along with n (Fig. 2a and 2b), respectively. The TFs under UV light irradiation (the inset of Fig. 2a and 2b) also reveal well-defined red and green luminescence with enhanced brightness upon increasing n. The fluorescence positions of the as-prepared TFs show no obvious red or blue shift upon the increasing bilayer numbers, suggesting the absence of LCs aggregates in the TFs throughout the whole assembly process. Additionally, the LC/LDHs TFs can also be fabricated on any desirable substrate (such as on flexible polymer as shown in Fig. 2c and 2d), which present the uniform red/green emission as those on the quartz. This guarantees their future applications in flexible optical displays.

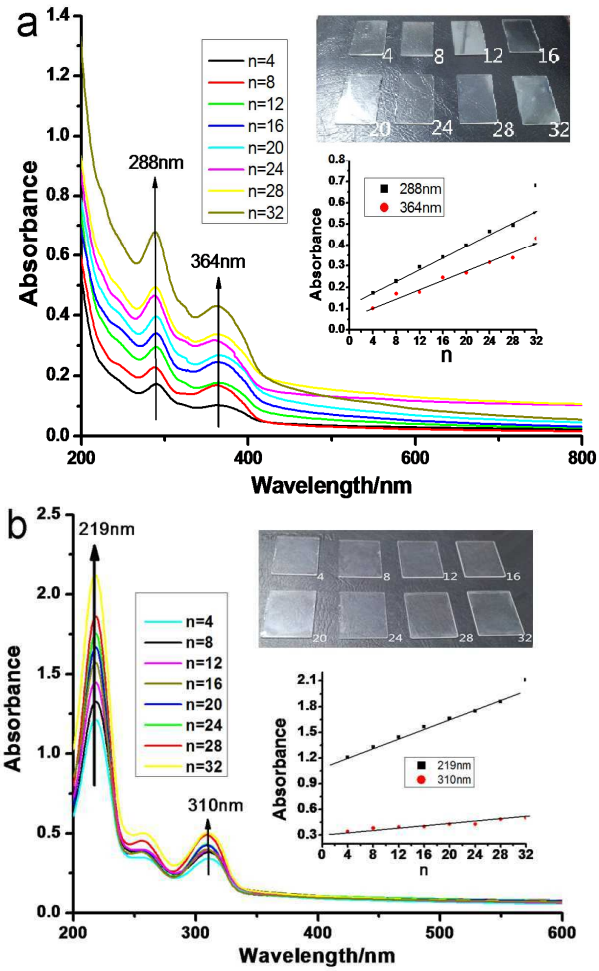

Fig. 1. UV–vis absorption spectra for a) (Eu(DBM)$_3$bath/LDH)$_n$ (n=4–32) TFs; b) (Tb(acac)$_3$Tiron/LDH)$_n$ (n=4–32) TFs. Insets show the plot of the absorbance intensity as a function of n, and photographs of TFs with different n when exposed to the daylight.

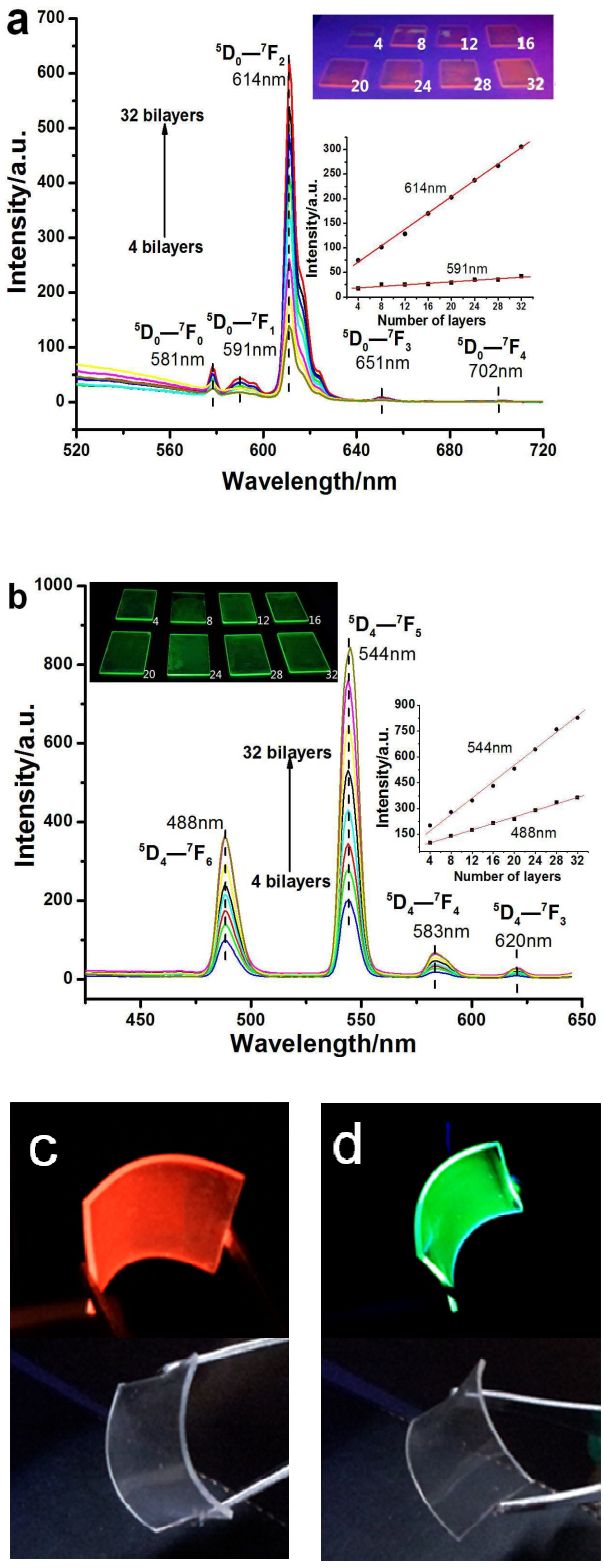

Fig. 2. Fluorescence spectra of a) $(Eu(DBM)_3bath/LDH)_n$ (n=4–32) TFs, b) $(Tb(acac)_3Tiron/LDH)_n$ (n=4–32) TFs and photographs of TFs with different n under UV light. c) and d) show the $(Eu(DBM)_3bath/LDH)_8$ and $(Tb(acac)_3Tiron/LDH)_8$ TFs fabricated on flexible polymer substrates.

3.3 Structural and morphological characterization of the hybrid LCs/LDH TFs.

X-ray diffraction was employed to detect the structure of the luminescent LCs/LDH TFs. X-ray diffraction patterns (Fig. S4 in ESI) of the $(Eu(DBM)_3bath/LDH)_n$ and $(Tb(acac)_3Tiron/LDH)_n$ TFs show the appearance of (001) reflection at *ca.* 2.4° and 2.6°, respectively, in which the reflection peak intensity increases with the increase of n. This indicates that the TFs possess a periodical structure in the normal direction of the film with a period of *ca.* 3.9 nm and 3.5 nm, respectively. These observations are also in agreement with the idealized structural models of the LCs/LDH systems in which the LCs anions adopt a parallel arrangement fashion relative to the LDH layers (Fig. S5a and S5b in ESI). To probe the surface morphology of the LC-based films, the $(LC/LDH)_n$ TFs were further detected by scanning electron microscopy and atomic force microscopy (SEM and AFM). The typical top-view SEM images for the $(LC/LDH)_n$ TFs (Fig. 3a and Fig. S6a in ESI) show that the film surface is continuous and homogeneous; the AFM images (Fig. S7 in ESI) reveal the root-mean square roughness of the TFs are in the range of 15.318-33.260 nm and 3.444-14.952 nm, respectively, indicating a relative smooth surface. Side-view SEM images (Fig. 3b and Fig. S6b in ESI) exhibit that the thickness of the $(Eu(DBM)_3bath/LDH)_n$ and $(Tb(acac)_3Tiron/LDH)_n$ TFs increase nearly linearly from 32 to 145 nm and from 26 to 120 nm (n = 8–32), respectively, further confirming the uniform and periodic structure of the LC-based TFs. These observations are also in agreement with the results revealed by UV-vis and fluorescence spectra described above. Moreover, the increase trend of the $(LC/LDH)_n$ TFs (Fig. 3b and Fig. S6b) indicate the thickness of one bilayer of $Eu(DBM)_3bath/LDH$ and $Tb(acac)_3Tiron/LDH$ unit are 4.53 nm and 3.75 nm, respectively, in consistent with those of the XRD result.

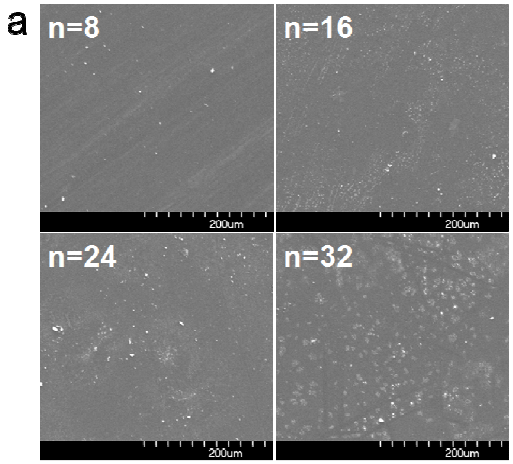

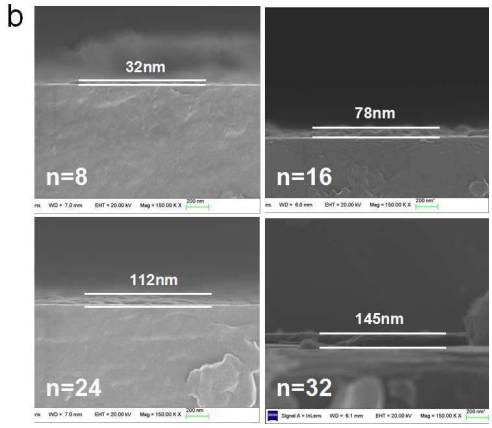

Fig. 3. The top (a) and side (b) view SEM profiles of the $(Eu(DBM)_3bath/LDH)_n$.

3.4 Photoluminescence quantum yield (PLQY), fluorescence lifetime and up-conversion emission of LC/LDH TFs.

To obtain insight into the excited-state information of fluorescence for LC/LDHs, the samples were studied by detecting their fluorescence decays (Fig. S8 in ESI). It can be shown that the PL lifetime of the LC/LDHs is enhanced compared with those of the solution and powder samples (Table S2 in ESI), and the lifetime values are at the level of the typical LC-based systems.[11] For example, the lifetime of $Eu(DBM)_3bath/LDH$ are in the range of 0.36-0.39 ms, which is larger than those in the solution (0.28 ms) and powder (0.27 ms) forms of $Eu(DBM)_3bath$. This can be attributed to the confined effect of LC within the LDH layer, which decreases the nonradiative relaxation of exciting states. Furthermore, the temperature dependence of the fluorescence lifetime was further detected (Table S3 in ESI), and it can be observed that the fluorescence decay of the LC/LDH TFs and LC solutions are obviously reduced with the increase of temperature, suggesting that the complex may undergo thermally activated back energy transfer. In addition, to detect the fluorescence efficiency of the TFs with different bilayers, the measurement on photoluminescence quantum yield (PLQY) was further made (Table S4 in ESI), it can be observed that the PLQY values are in the range of 6.1%-7.8% and 8.2%-10.7% respectively for $Eu(DBM)_3bath/LDH$ and $Tb(acac)_3Tiron/LDH$ systems, in which the PLQY values have slightly increased upon the increasing number of layers. The PLQY values for $Eu(DBM)_3bath/LDH$ are slightly lower than the other reported system,[5b] and this may be related to the self-absorption of the films.

To develop potential up-conversion fluorescent materials based on the ordered LC systems, the $Eu(DBM)_3bath/LDH$ and $Tb(acac)_3Tiron/LDH$ TFs were further excited by an 800 nm laser with different excitation power (Fig. 4) It was observed that the two TFs with n=50 exhibited obvious red and green emission without emissive shift compared with those excited by UV light. Moreover, the log (intensity) *vs.* log (incident energy) present a good linear relationship, with the slop of 1.841 and 1.897 respectively for the $Eu(DBM)_3bath/LDH$ and $Tb(acac)_3Tiron/LDH$ systems. The two slops are close to 2, suggesting that the process may involve a two-photon mechanism. In this case, this is a conventional two-photon absorption induced fluorescence process, and two photons of 800 nm were simultaneously absorbed[12].

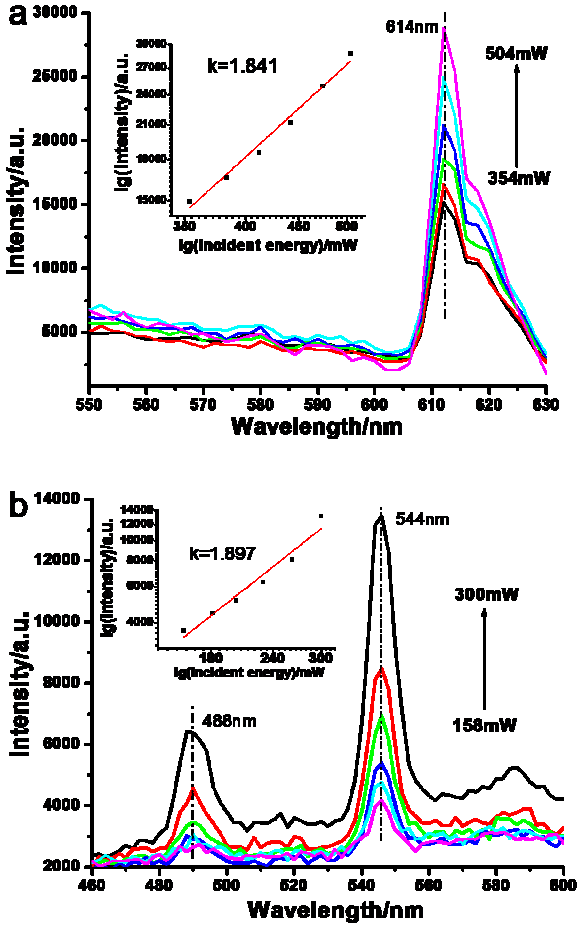

Fig. 4. Fluorescence spectra of a) $(Eu(DBM)_3bath/LDH)_{50}$ and b) $(Tb(acac)_3Tiron/LDH)_{50}$ excited by a 800 nm laser.

3.5 Fabrication of the two-color LCs/LDH TFs.

Based on the above single-color emission of two LC/LDH TFs, we have further fabricated the two-color red/green luminescent TFs. Such films can be prepared in a heterogeneous structure by the alternate deposition of one type of TF onto the surface of a different as-prepared TF. Taking $(Eu(DBM)_3bath/LDH)_{10}/(Tb(acac)_3Tiron/LDH)_n$ (n=0–14) as an example, UV-vis spectra show that the ratio of the absorption intensity at 219 nm to that at 371 nm correlates linearly with n (Fig. S9a in ESI), indicating a stepwise and regular growth of the $Tb(acac)_3Tiron/LDH$ units on the $Eu(DBM)_3bath/LDH$ TF. Fluorescence spectra show that the intensities of characteristic peaks of the $(Tb(acac)_3Tiron/LDH)_n$ (n=2–14) TFs at 544 nm display a monotonic increase with n, whereas the luminescence peak at 614 nm attributed to the pristine $(Eu(DBM)_3bath/LDH)_{10}$ maintain nearly the same intensity (Fig. 5a), suggesting that there is no energy transfer between the $Tb(acac)_3Tiron/LDH$ and $Eu(DBM)_3bath/LDH$ building blocks. In addition, the two-color emission can also be constructed by the co-assembly of mixture solutions of $Eu(DBM)_3bath$ and $Tb(acac)_3Tiron$ with LDH

nanosheets as indicated by the UV-vis spectra (Fig. S9b in ESI). Fig. 5b shows the fluorescent spectra of the $Eu(DBM)_3bath$@$Tb(acac)_3Tiron$/LDH TFs with the molar ratio of $Eu(DBM)_3bath$ to $Tb(acac)_3Tiron$ (c) in the range 0%–35%, in which the fluorescence intensity ratio I_{614}/I_{544} display a monotonic increase with c, accompanied with the change in the emissive color of the TFs (inset in Fig. 5).

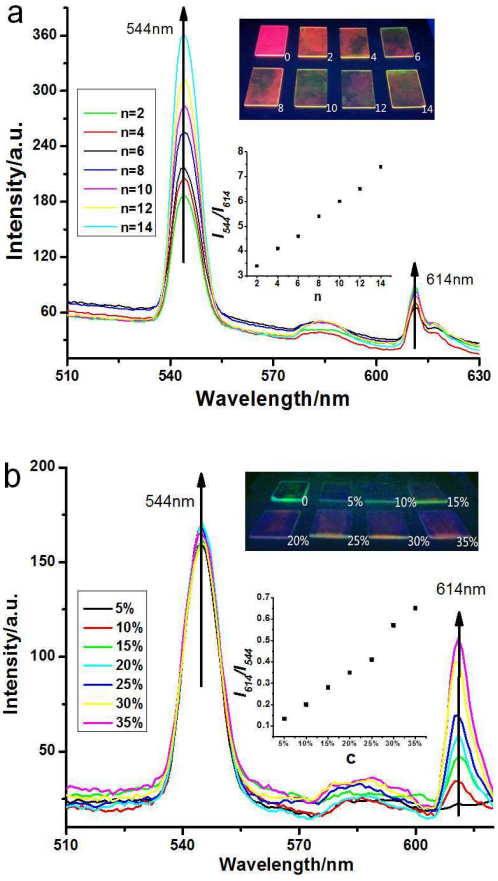

Fig. 5. a) $(Eu(DBM)_3bath/LDH)_{10}/(Tb(acac)_3Tiron/LDH)_n$ (n=0–14); b) different $Eu(DBM)_3bath$@$Tb(acac)_3Tiron$/LDH (c=0%–35%). Insets show the dependence of I_{544}/I_{614} on n and I_{614}/I_{544} on c, and photographs of corresponding TFs under UV light.

3.6 One- and two-color polarized luminescence.

The orderly structures of the LC/LDH TFs inspired us to exploit their polarized luminescent properties, and the glancing incidence geometry was employed to determine the luminescence anisotropy value r.[13a,b] The $Eu(DBM)_3bath$/LDH TFs show well-defined photoemission between the parallel and perpendicular to the excitation polarized direction (I_{VV} *vs.* I_{VH}) with the anisotropic value (r) of 0.103–0.145 around 614 nm (Fig. 6a), while the $Tb(acac)_3Tiron$/LDH TFs present the r value in the range of 0.205–0.249 near 544 nm (Fig. 6b). Furthermore, the r value is nearly independent on n as shown inset in Fig. 6. This indicates that the film thickness imposes no obvious influence on macroscopic polarized luminescence of TFs throughout the whole assembly process. To the best of our knowledge, very few LC-based materials have exhibited polarized luminescence due to their pseudo-spherical structures.[13c] In this work, the high r may be attributed to the regular alignment of LC anions between LDH monolayers.

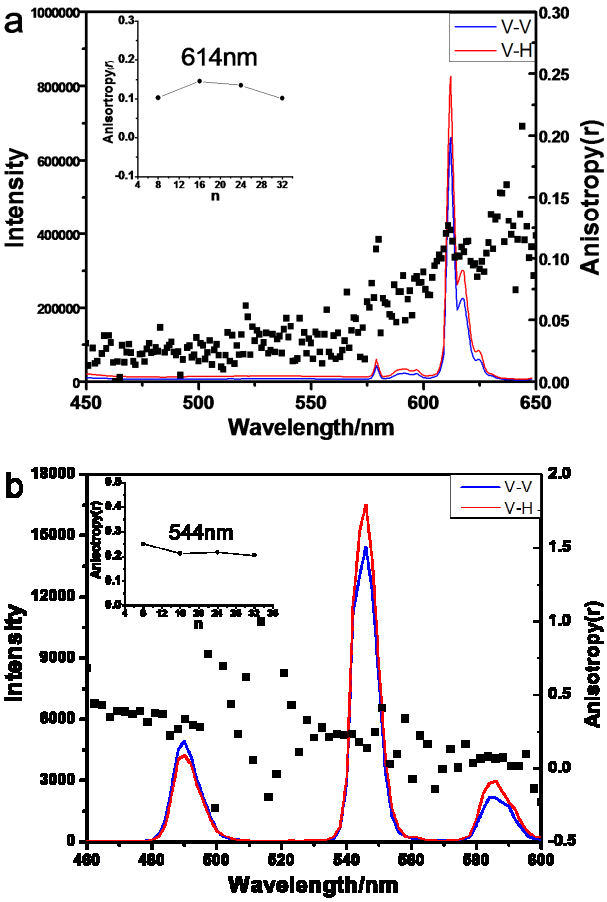

Fig. 6. The polarized fluorescence spectra for the $(LC/LDH)_n$ TFs. a) $(Eu(DBM)_3bath/LDH)_8$; b) $(Tb(acac)_3Tiron/LDH)_8$ (the insets show the plots of the anisotropic value as a function of n).

For the two-color LC/LDH systems, polarized luminescence measurement (Fig. S10) further shows that the r values at red and green wavelengths has no obvious change compared with their corresponding single-color emissive TFs. Furthermore, the effect of bilayer number on the polarized luminescence of the TFs was studied. The results (inset of Fig. 6 and Fig. S10) show that the film thickness only has slight influence on the macroscopic polarized luminescence characteristics of TFs, which is indicative of an ordered assembly of the TFs. Such observation is consistent with the XRD results. It is anticipate that such two-color polarized luminescent TFs can be applied as color-switchable film materials in display devices.

4. Conclusion.

In summary, the ordered LC-based TFs were constructed by LBL deposition of sulfonated LCs and LDH nanosheets, which show periodic long-range order structure, well-defined polarized red/green photoemission and up-conversion luminescence. The two-color emission with tunable red/green emissive intensity can also be achieved by tailoring the assembly procedure and concentration ratios of the LC units

within the films. To the best of our knowledge, this work may involve the first example of the LC-based TFs with polarized emission, tunable two-color fluorescence and up-conversion luminescence. It can be expected that, by designing and tuning the component, diversity and alignment of anionic LCs within the LDH layers, the LC-based TFs can be readily extended and applicable to other similar systems, which have much potential applications for the design of various LC-based optical films and devices.

Acknowledgment.

This work was supported by the 973 Program (Grant no. 2014CB932103), the 863 Program (Grant No. 2013AA032501), the National Natural Science Foundation of China (NSFC), the Scientific Fund from Beijing Municipal Commission of Education (20111001002), the Fundamental Research Funds for the Central Universities, the 111 Project (Grant B07004), and Program for Changjiang Scholars and the Innovative Research Team in University (PCSIRT: IRT1205).

Notes and references

[a] *State Key Laboratory of Chemical Resource Engineering, Beijing University of Chemical Technology, Beijing 100029, P. R. China Fax: +86-10-64425385; Tel: +86-1064412131; Email : yandongpeng001@163.com; yandp@mail.buct.edu.cn*
[b] *Key Laboratory of Theoretical and Computational Photochemistry, Ministry of Education, College of Chemistry, Beijing Normal University, Beijing 100875, P. R. China*
[c] *College of Chemistry and Molecular Engineering, Peking University, Beijing, 100871, P. R. China.*

† *Electronic Supplementary Information (ESI) available: [characterization of LC and LC/LDH)$_n$]. See DOI: 10.1039/b000000x/*

1 a) O. Bolton, K. Lee, H. J. Kim, K. Y. Lin an, *Nat. Chem*., 2011, **3**, 205; b) A. Kohler, J. S. Wilson and R. H. Friend, *Adv. Mater*., 2002, **14**, 701; c) D. V. Talapin, J. S. Lee, M. V. Kovalenko and E. V. Shevchenko, *Chem. Rev*., 2010, **110**, 389.

2 a) L. D. Carlos, R. A. S. Ferreira, V. d. Z. Bermudez and S. J. L. Ribeiro, *Adv. Mater*., 2008, **20**, 1; b) C. Feldmann, T. Justel, C. R. Ronda and P. J. Schmidt, *Adv. Funct. Mater*., 2003, **13**, 511; c) H. Tsukube and S. Shinoda, *Chem. Rev*., 2002, **102**, 2389.

3 a) JCG. Bünzli and C. Piguet, *Chem. Soc. Rev*., 2005, **34**, 1049; b) J. Kido and Y. Okamoto, *Chem. Rev*., 2002, **102**, 2357. c) G. J. C. Bünzli and C. Piguet, *Chem. Rev*., 2002, **102**, 1897. d) Z. Liu, W. He and Z. Guo, *Chem. Soc. Rev*., 2013, **42**, 1568.

4 a) X Gao, M Hu, L Lei, D O'Hare, C Markland, Y Sun and F. Stephen, *Chem. Commun*., 2011, **47**, 2104; b) J Wang, J Zhou, Z Li, Y Song, Q Liu, Z. Jiang and M. Zhang, *Chem. Eur. J*, 2010, **16,** 14404; c) D. Yan, J. Lu, M. Wei, J. Han, J. Ma, F. Li, D. G. Evans and X. Duan, *Angew. Chem. Int. Ed*., 2009, **48**, 3073.

5 a) F. Vetrone, R. Naccache, V. Mahalingam, C. G. Morgan and J. A. Capobianco, *Adv. Funct. Mater*., 2009, **19**, 2924; b) S. D. Meetei, S. D. Singh, *J. Lumin.,* 2014, **147**, 328; c) T. Wen, W. Luo, Y. Wang, M. Zhang, Y. Guo, J. Yuan, J. Ju, Y. Wang, F. Liao and B. Yang, *J. Mater. Chem. C*, 2013, **1**, 1995; d) P. Gunawan and R. Xu, *J. Phys. Chem. C*, 2009, **113**, 17206; e) J. Yang, Q. Yue, G. Li, J. Cao, G. Li and J. Chen, *Inorg. Chem*., 2006, **45**, 2858; f) J. Xu, S. Zhao, Z. Han, X. Wang and Y. F. Song, *Chem. Eur. J*, 2011, **17**, 10365.

6 a) L. N. Sun, H. J. Zhang, Q. G. Meng, F. Y. Liu, L. S. Fu, C. Y. Peng, J. B. Yu, G. L. Zheng and S. B. Wang, *J. Phys. Chem. B*, 2005, **109**, 6174; b) J. Zhang, P. D. Badger, S. J. Geib and S. Petoud, *Angew. Chem. Int. Ed.,* 2005, **44**, 2508. c) A. de Bettencourt-Dias, *Dalton Trans.*, 2007, 2229. d) L. Zhou, Z. Gu, X. Liu, W. Yin, G. Tian, L. Yan, S. Jin, W. L. Ren, G. M Xing, W. Li, X. L. Chang, Z. B. Hu and Y. L. Zhao, *J. Mater. Chem.*, 2012, **22**, 966.

7 a) A. M. Fogg, A. J. Freij and G. M. Parkinson, *Chem. Mater*., 2002, **14**, 232; b) J. H. Choy, S. Y. Kwak, J. S. Park and Y. J. Jeong, *Adv. Funct. Mater*., 2012, **22**, 4940; c) S. Gago, T. Costa, J. S. De Melo, I. S. Gonçalves and M. Pillinger, *J. Mater. Chem*., 2008, **18**, 894; d) H. Y. Ma, R. Gao, D. P. Yan, J. W. Zhao and M. Wei, *J. Mater. Chem. C*, 2013, **1**, 4128; e) D. P. Yan, J. Lu, J. Ma, M. Wei, S. H. Qin, L. Chen, D. G. Evans and X. Duan, *J. Mater. Chem*., 2010, **20**, 5016.

8 a) A. I. Khan, L. X. Lei, A. J. Norquist and D. O'Hare, *Chem. Commun*., 2001, 2342; b) L. Li, R. Z. Ma, N. Iyi, Y. Ebina, K. Takada and T. Sasaki, *Chem. Commun*., 2006, 3125; c) X. Guo, F. Zhang, D. G. Evans and X. Duan, *Chem. Commun*., 2010, **46**, 5197; d) C. A. Antonyraj, P. Koilraj and S. Kannan, *Chem. Commun*., 2010, **46**, 1902; e) Q. Wang and D. O'Hare, *Chem. Rev*., 2002, **112**, 4124; f) D. P. Yan, J. Lu, M. Wei, D. G. Evans and X. Duan, *J. Mater. Chem*., 2011, **21**, 13128; g) D. G. Evans and X. Duan, *Chem. Commun*., 2006, 485; h) C. Chen, P. Gunawan, X. W. Lou and R. Xu, *Adv. Funct. Mater*., 2012, **22**, 780; i) J.-H. Choy, S.-Y. Kwak, Y.-J. Jeoing and J.-S. Park, *Angew. Chem. Int. Ed*., 2000, **39**, 4041.

9 a) D. P. Yan, J. Lu, M. Wei, S. H. Qin, L. Chen, S. Zhang, D. G. Evans and X. Duan, *Adv. Funct. Mater*., 2011, **21**, 2497; b) D. Yan, J. Lu, M. Wei, J. Ma, D.G. Evans and X. Duan, *Chem. Commun*., 2009, 6358; c) D. Yan, J. Lu, J. Ma, M. Wei, D. G. Evans and X. Duan, *Angew. Chem. Int. Ed*., 2011, **50**, 720; d) D. P. Yan, G. O. Lloyd, A. Delori, W. Jones and X. Duan, *ChemPlusChem*, 2012, **77**, 1112; (e) D. P. Yan, R. Gao, M. Wei, S. D. Li, J. Lu, D. G. Evans and X. Duan, *J. Mater. Chem. C*, 2013, **1**, 997.

10 D. P. Yan, J. Lu, M. Wei, J. B. Han, J. Ma, F. Li, D. G. Evans and X. Duan, *Angew. Chem. Int. Ed*., 2009, **48**, 3073.

11 M. H. V. Werts, R. T. F. Jukes and J. W. Verhoeven, *Phys. Chem. Chem. Phys.,* 2002, **4**, 1545.

12 a) M. H. V. Werts, N. Nerambourg, D. Pélégry, Y. L. Grandb and M. Blanchard-Desce, *Photochem. Photobiol. Sci.*, 2005, **4**, 531; b) G. Chen, H. Qiu, P. N. Prasad and X. Chen, *Chem. Rev.*, 2014, **10**, 5161.

13 a) $r = (I_{vv}–GI_{VH})/(I_{vv} + 2GI_{VH})$, where $G = I_{HV}/I_{HH}$, determined from the aqueous solution. I_{VH}: the emission intensity with vertical polarization excitation and horizontal polarization detection, and I_{VH}, I_{VH}, I_{VH} are defined in a similar way; b) D. Yan, J. Lu, M. Wei, J. Ma, D. G. Evans and X. Duan, *Phys. Chem. Chem. Phys.,* 2009, **11**, 9200; c) Y. G. Galyametdinov, A. A. Knyazev, V. I. Dzhabarov, T. Cardinaels, K. Driesen, C. Gorller-Walrand and K. Binnemans, *Adv. Mater.,* 2008, **20**, 252; d) T. Q. Nguyen, J. J. Wu, V. Doan, B. J. Schwartz and S. H. Tolbert, *Science*, 2000, **288**, 652.

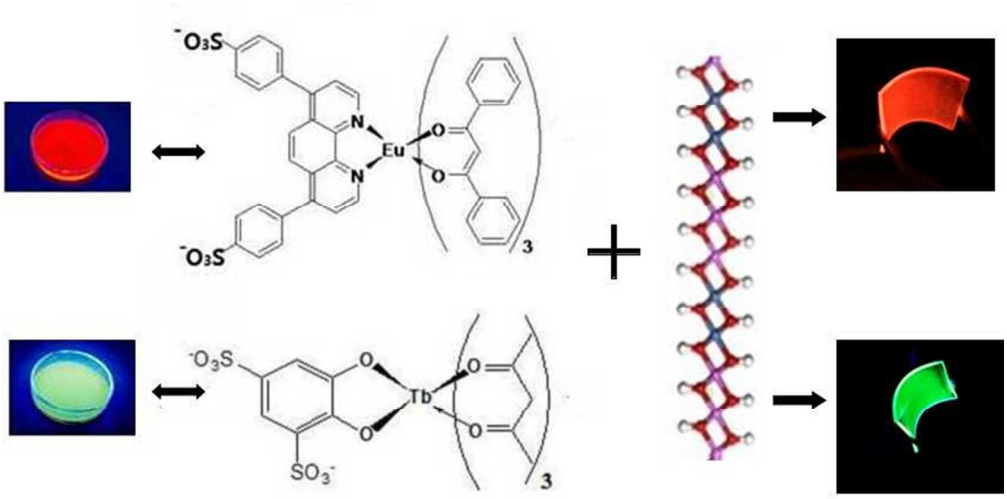

The ordered transparent thin films based on alternate layer-by-layer assembly of lanthanide complexes and layered double hydroxide nanosheets have been fabricated, which exhibit up-conversion emission and tunable two-color luminescence.
225x114mm (96 x 96 DPI)